MCB
Journals.ASM.org

Saccharomyces cerevisiae Ribosomal Protein L26 Is Not Essential for Ribosome Assembly and Function

Reyes Babiano,[a] Michael Gamalinda,[b] John L. Woolford, Jr.,[b] and Jesús de la Cruz[a]

Departamento de Genética, Universidad de Sevilla, Seville, Spain,[a] and Department of Biological Sciences, Carnegie Mellon University, Pittsburgh, Pennsylvania, USA[b]

Ribosomal proteins play important roles in ribosome biogenesis and function. Here, we study the evolutionarily conserved L26 in *Saccharomyces cerevisiae*, which assembles into pre-60S ribosomal particles in the nucle(ol)us. Yeast L26 is one of the many ribosomal proteins encoded by two functional genes. We have disrupted both genes; surprisingly, the growth of the resulting *rpl26* null mutant is apparently identical to that of the isogenic wild-type strain. The absence of L26 minimally alters 60S ribosomal subunit biogenesis. Polysome analysis revealed the appearance of half-mers. Analysis of pre-rRNA processing indicated that L26 is mainly required to optimize 27S pre-rRNA maturation, without which the release of pre-60S particles from the nucle(ol)us is partially impaired. Ribosomes lacking L26 exhibit differential reactivity to dimethylsulfate in domain I of 25S/5.8S rRNAs but apparently are able to support translation *in vivo* with wild-type accuracy. The bacterial homologue of yeast L26, L24, is a primary rRNA binding protein required for 50S ribosomal subunit assembly *in vitro* and *in vivo*. Our results underscore potential differences between prokaryotic and eukaryotic ribosome assembly. We discuss the reasons why yeast L26 plays such an apparently nonessential role in the cell.

Elucidation of the crystal structure of both prokaryotic and eukaryotic ribosomes at atomic resolution (for examples, see references 7, 98, and 113 and references therein) has confirmed that ribosome assembly must be an extremely complex process. Pioneering work of Nomura and Nierhaus in the 1970s established that bacterial ribosomal subunits (r-subunits) could be reconstituted *in vitro* from mature ribosomal RNAs (rRNAs) and r-proteins (40, 41, 65, 69, 70). These experiments demonstrated that r-subunits assemble in a cooperative and hierarchical manner through reconstitution intermediates (for reviews, see references 46 and 93). Hence, the r-proteins were classified as primary binding or assembly initiator proteins, which bind directly to rRNA, and secondary and tertiary binding proteins, which require prior binding of one or more r-proteins. More recent work has demonstrated that bacterial ribosome assembly *in vitro* occurs via multiple parallel pathways (68, 99, 101). The extent to which bacterial ribosome assembly pathways *in vivo* resemble the *in vitro* reconstitution experiments remains unclear for a number of reasons. (i) Assembly is much faster and more efficient *in vivo*, taking less than 3 min during bacterial exponential growth versus the 30 to 120 min for the *in vitro* reconstitution experiments (93). (ii) Assembly is cotranscriptional *in vivo* (17, 77). (iii) Assembly occurs *in vivo* with the primary pre-rRNA transcript, which contains spacer sequences, while *in vitro* reconstitution experiments are done with mature rRNAs. (iv) Ribosome assembly *in vivo* requires dozens of *trans*-acting factors, such as exo- and endonucleases, RNA helicases, GTPases, chaperones, and rRNA- and r-protein-modifying enzymes (reviewed in references 13 and 93). (v) The composition of the *in vivo* precursor particles is not identical to *in vitro* reconstitution intermediates but exhibits some degree of similarity (69, 93). (vi) Other discrepancies were found between *in vivo* and *in vitro* ribosome assembly. For instance, r-protein S15, which is a primary binding protein required for binding of four other 30S r-proteins in reconstitution assays, is dispensable *in vivo* (9).

Much less is known about the details of eukaryotic ribosome assembly. To date, *in vitro* reconstitution of both functional 40S and 60S r-subunits has been achieved only in the social amoeba *Dictyostelium discoideum* (62). Nevertheless, assembly maps are lacking. The process of r-subunit assembly *in vivo* is also poorly understood. Assembly *in vivo* occurs concomitantly with processing and modification of the pre-rRNAs, which are well-defined pathways (see Fig. S1 in the supplemental material). By far, ribosome biogenesis has been best studied in the yeast *Saccharomyces cerevisiae*. Ribosome synthesis proceeds via the formation of preribosomal intermediates that contain r-proteins and many nonribosomal proteins, so-called ribosome assembly or *trans*-acting factors, which likely provide this process with the necessary speed, accuracy, and directionality (for examples, see references 37, 71, and 91; reviewed in references 31 and 53). The preribosomal intermediates are termed, according to their position in the ribosome assembly pathway, 90S preribosomal particles, nuclear and cytoplasmic 43S preribosomal particles, and early, intermediate, late, and cytoplasmic pre-60S r-particles (16, 21, 31, 103). The complexity of the different particles decreases during their maturation to r-subunits, while concomitant structural rearrangements allow the stable incorporation of all r-proteins. Insights into the approximate timing of association and dissociation of some of the protein ribosome biogenesis factors have been obtained by studying the composition of distinct pre-60S complexes purified from wild-type cells (reviewed in references 31 and 53) and from mutant strains blocked at early, intermediate, or late

Received 25 April 2012 Returned for modification 21 May 2012
Accepted 1 June 2012
Published ahead of print 11 June 2012
Address correspondence to John L. Woolford, Jr., jw17@andrew.cmu.edu, or Jesús de la Cruz, jdlcd@us.es.
We dedicate this article to the memory of Pierre Thuriaux.
R.B. and M.G. contributed equally to this work.
Supplemental material for this article may be found at http://mcb.asm.org/.

doi:10.1128/MCB.00539-12

nuclear steps of ribosome maturation (for examples, see references 56 and 90 and references therein). However, the course of the assembly of the r-proteins has not been reported with much precision. Low-resolution pictures of early and late r-protein assembly have been obtained by monitoring the kinetics of *in vivo* incorporation of labeled r-proteins into preribosomal particles and cytoplasmic r-subunits (54). More recent investigations have analyzed the incorporation of yeast 40S r-proteins into 90S and 43S preribosomal particles (30), which have allowed the identification of some principles governing the assembly of the 40S r-subunits and the establishment of a certain parallelism between the *in vivo* assembly of 40S r-subunits and the *in vitro* reconstitution data of bacterial 30S r-subunits (30). However, the relative timing of the assembly of only a few 60S r-proteins has been investigated (4, 45, 84, 87, 90, 112).

We want to understand the contribution of 60S r-proteins to ribosome biogenesis, specifically the role of these proteins in driving the formation and/or rearrangements of preribosomal particles. Previously, a systematic analysis of the role of 26 essential yeast 60S r-proteins in pre-rRNA processing and nucleocytoplasmic transport of pre-60S r-particles was performed (78). Before this analysis, the contribution to ribosome biogenesis of only a few 60S r-proteins was studied in some detail (for examples, see references 4, 18, 19, 45, 63, 84, 85, 87, and 106). In this report, we have undertaken the functional analysis of yeast L26 in the biogenesis and function of ribosomes which remained uncharacterized. Eukaryotic L26 is a conserved protein that shares notable sequence and structure identity with archaeal and eubacterial L24. L24 is one of two initiator r-proteins for assembly of 50S r-subunits *in vitro* (69). Our results clearly show that yeast L26 assembles in the nucle(ol)us within the earliest assembly intermediates but makes very minor contributions to the biogenesis, structure, and function of 60S r-subunits. Consequently, L26 is apparently dispensable for cell growth under standard laboratory conditions.

MATERIALS AND METHODS

Strains and microbiological methods. The yeast strains used in this study are listed in Table S1 in the supplemental material. Strains RBY272 and RBY274 are haploid segregants of Y25253 and Y24664 (Euroscarf), respectively. Strain RBY276 is a haploid segregant derived from crossing RBY272 and RBY275, which is another segregant of Y25253. Deletion disruption, *GAL* constructs, and C-terminal TAP or Myc tagging at the genomic loci of the yeast JWY6147 were performed as described previously (39, 61, 78, 81, 110).

Growth and handling of yeast strains and preparation of standard media were performed by established procedures (47). Rich medium (1% yeast extract, 2% peptone; YP) or synthetic (S) minimal medium (0.15% yeast nitrogen base, 0.5% ammonium sulfate) were supplemented with the appropriate amino acids and bases as nutritional requirements and with 2% galactose (YPGal and SGal, respectively), 2% glucose (YP-dextrose [YPD] and SD, respectively), or 2% raffinose (SRaf). Unless otherwise indicated, yeast cells were grown at 30°C to an optical density at 600 nm (OD_{600}) of about 0.8. All solid media contained 2% agar. Low-pH methylene blue plates were prepared according to a standard procedure (47).

Plasmids. All recombinant DNA techniques were performed according to established procedures using *Escherichia coli* DH5α for cloning and plasmid propagation (88). The plasmids used in this study are described listed in Table S2 in the supplemental material.

Sucrose gradient centrifugation. Polysome preparations and analyses were performed as previously described (52) using an ISCO UA-6 system equipped to continuously monitor the A_{254}.

Pulse-chase labeling of pre-rRNA. Pulse-chase labeling of pre-rRNA was performed as previously described (52), using 100 μCi of [5,6-^{3}H] uracil (45 to 50 Ci/mmol; Perkin Elmer) per 40 OD_{600} units of yeast cells. Cells were first transformed with an empty YCplac33 plasmid (*CEN URA3*) (see Table S2 in the supplemental material) to make them prototrophic for uracil. They were grown in liquid SD-Ura medium to exponential growth phase, pulse-labeled for 2 min, and chased for 5, 15, 30, and 60 min with an excess of cold uracil. Total RNA was extracted by the acid-phenol method (3). About 20,000 cpm per RNA sample were analyzed both in 1.2% agarose–6% formaldehyde and 7% polyacrylamide–8 M urea gels. RNA then was transferred to a nylon membrane and visualized by fluorography (52).

Northern hybridization and primer extension analyses. Steady-state levels of pre-rRNAs were assessed by Northern and primer extension analyses as described previously (107). In all experiments, RNA was extracted from samples corresponding to 10 OD_{600} units of exponentially grown cells. Equal amounts of total RNA (5 μg) were loaded on gels or used for primer extension reactions. Specific oligonucleotides, whose sequences are listed in Table S3 in the supplemental material, were 5′ end labeled with [γ-^{32}P]ATP and used as probes. To analyze mRNAs, double-stranded DNA probes were generated by random priming of a PCR fragment of the *RPL26A* and *RPL26B*, *RPL35A* and *RPL35B*, and *ADH1* genes with [^{32}P]dCTP. The sequences of the oligonucleotides used as primers for the PCRs are also listed in Table S3.

Fluorescence microscopy. To test preribosomal particle export, the appropriate strains were cotransformed with pRS316 plasmid constructs (gifts from J. Bassler), which express the nucleolar marker mRFP-Nop1 and either the L25-enhanced green fluorescent protein (L25-eGFP) or the S3-eGFP reporter (105). Several transformants then were grown to mid-log phase in selective SD liquid medium, washed, and resuspended in sterile distilled water. To address the assembly position of L26, the *rpl26* null strain was cotransformed with YCplac111-RPL26A-eGFP and the pRS316-*GAL-NMD3Δ100* or the pRS316-*GAL-NMD3FL* plasmid (gifts from A. Jacobson). These plasmids express a dominant-negative truncation or a wild-type allele of the *NMD3* gene, respectively, under the control of an inducible *GAL* promoter (6). Transformants were grown in selective SRaf medium and shifted to selective SGal medium to induce the expression of the Nmd3 proteins. Image acquisition was done in a Leica DMR microscope equipped with a differential contrast (DC) camera. Digital images were processed with Adobe Photoshop 7.0.

Preparation of ribosome particles. Ribosomes were obtained as previously described (83). Briefly, 200 ml of wild-type or *rpl26* null cells was grown in YPD to an OD_{600} of 0.8 and concentrated in 500 μl of ice-cold buffer 1 (10 mM Tris-HCl, pH 7.4; 20 mM KCl; 12.5 mM $MgCl_2$; 5 mM 2-mercaptoethanol) containing a protease inhibitor cocktail. Cells were disrupted by vigorous shaking with glass beads in a Fastprep-24 homogenizer at 4°C. An S30 fraction was obtained by centrifuging the extract at 13,000 rpm for 20 min at 4°C in an Eppendorf microcentrifuge. Ribosomal particles were prepared from the S30 fraction by centrifugation in a Beckman-Coulter Optima Max using a TL110 rotor at 90,000 rpm for 90 min at 4°C. The particles were washed by centrifugation in a 20 to 40% discontinuous sucrose gradient in buffer 2 (20 mM Tris-HCl, pH 7.4; 500 mM ammonium acetate; 100 mM $MgCl_2$; 5 mM 2-mercaptoethanol) and stored at −80°C in the same buffer. Ribosomal proteins were separated in NuPAGE-SDS with 4 to 12% gradient polyacrylamide gels (Invitrogen), and the indicated proteins were assayed by Western blotting.

Translational *in vivo* assays. (i) The sensitivity to different drugs impairing translation was tested as follows. Wild-type and *rpl26* null strains were grown in YPD medium to an OD_{600} of 0.8 and diluted to an OD_{600} of 0.05. A series of 10-fold dilutions was done for each strain, and 5-μl drops were spotted on YPD plates containing the following antibiotics at the concentrations specified: anisomycin (15 μg/ml), azetidine-2-carboxylic acid (AZC; 0.5 mg/ml), cycloheximide (0.1 μg/ml), hygromycin B (20 μg/ml), paramomycin (2.5 mg/ml), and neomycin (5 mg/ml).

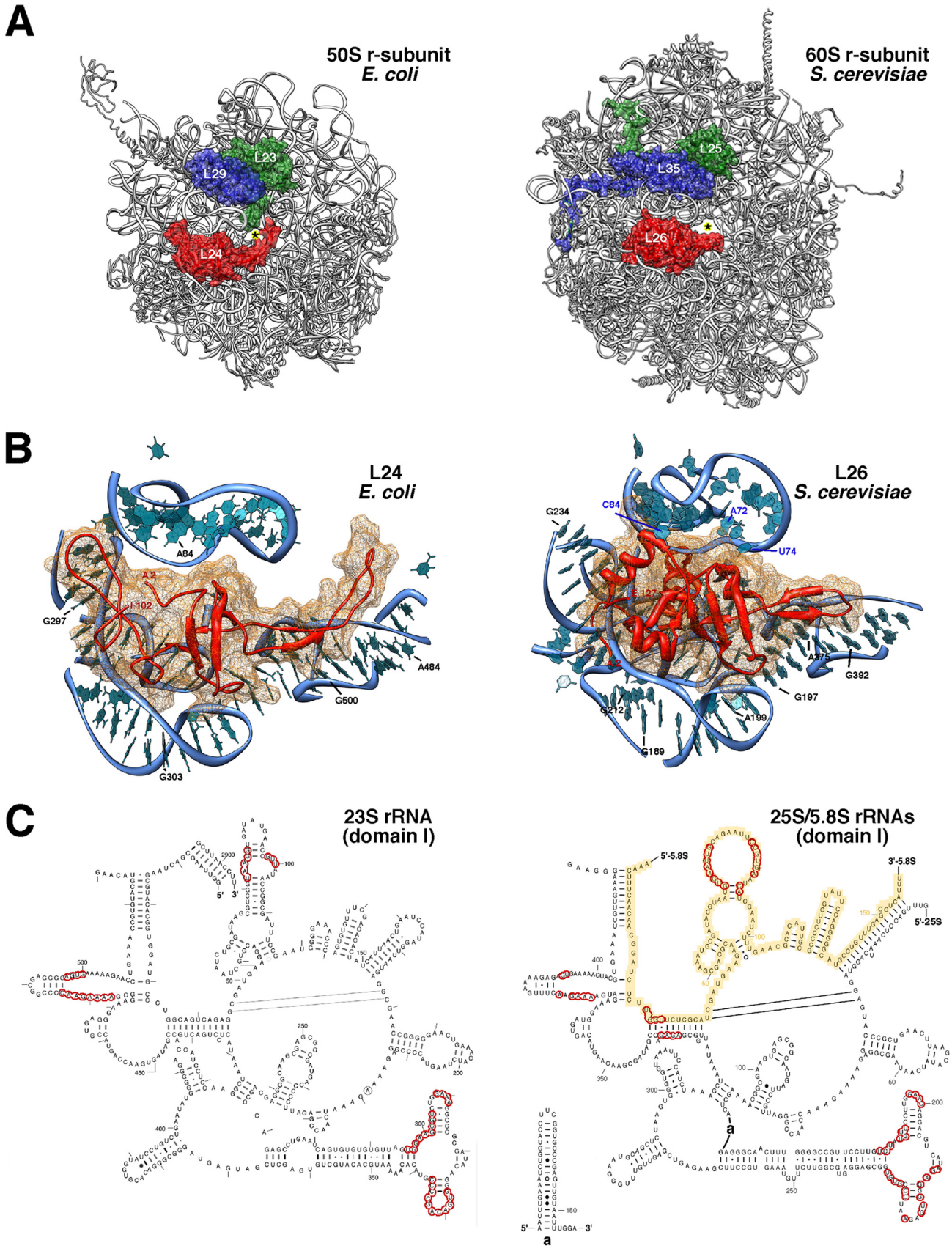
A
50S r-subunit
E. coli
L23
L29
L24
60S r-subunit
S. cerevisiae
L25
L35
L26
B
L24
E. coli
A84
A2
L 102
G297
A484
G500
G303
L26
S. cerevisiae
G234
C84
A72
U74
L 127
A375
G392
G197
G212
A189
G189
C
23S rRNA
(domain I)
5' 3'
25S/5.8S rRNAs
(domain I)
5'-5.8S
3'-5.8S
5'-25S
a
5'
3'

Plates were incubated at 30°C for 3 to 4 days. (ii) The killer virus assay was carried out exactly as described in reference 47. Briefly, yeast colonies were replica plated to low-pH methylene blue plates freshly inoculated with 0.2 ml of an overnight culture of the sensitive 5X47 strain and incubated for 4 days at 16 or 20°C. The killer activity was scored as a zone of growth inhibition around the killer colonies. (iii) To monitor programmed +1 and −1 frameshifting (PRF), plasmids p0-LacZ, p-1-LacZ, and p+1-LacZ (gifts from J. D. Dinman) were used exactly as described previously (22, 23). Plasmid p0-LacZ carries a *lacZ* gene expressed from a *PGK1* promoter. Plasmid p-1-LacZ carries an L-A-derived −1 r-frameshift sequence inserted in the *lacZ* gene. Plasmid p+1-LacZ carries a Ty1-derived +1 r-frameshift sequence inserted in the *lacZ* gene. Wild-type and *rpl26* null cells were transformed with these plasmids and analyzed for β-galactosidase activity (59). The efficiency of PRF correlates with the β-galactosidase activity produced by cells harboring p-1-LacZ or p+1-LacZ relative to that produced by cells harboring p0-LacZ. All assays were performed for at least three independent transformants of each plasmid in triplicate. (iv) To monitor readthrough activity, wild-type and *rpl26* null cells were transformed with pUKC815, pUKC817, pUKC818, and pUKC819 plasmids (gifts from M. Tuite) (104). pUKC815 carries a *lacZ* gene expressed from a *PGK1* promoter and is used as a β-galactosidase activity standard. Expression of β-galactosidase activity from pUKC817, pUKC818, and pUKC819 requires readthrough of the UAA, UAG, and UGA codons, respectively. As described above, β-galactosidase activity was assayed for three independent transformants of each plasmid in triplicate. (v) To assay the stringency in start codon selection, wild-type and *rpl26* null cells were transformed with p367 and p391 plasmids (gifts from A. Hinnebusch) (12). Plasmid p367 carries a *HIS4*^{AUG}*-lacZ* fusion; p391 is a derivative of p367, with UGG as the first codon of the *HIS4-lacZ* open reading frame (ORF) (*HIS4*^{UUG}*-lacZ*). As described above, β-galactosidase activity was assayed for three independent transformants of each plasmid in triplicate.

Affinity purification of preribosomal particles. Preribosomal complexes were affinity purified from whole-cell extracts with magnetic Dynabeads (Invitrogen), using tandem affinity purification (TAP)-tagged Nop7 assembly factor as bait, exactly as described in previous reports (72, 87). Purified proteins were precipitated in 10% trichloroacetic acid, subsequently resuspended in SDS Laemmli sample buffer, and separated by SDS-PAGE in 4 to 20% polyacrylamide Novex gels (Invitrogen). Proteins then were visualized by silver staining or Western blotting. Western blotting was done using a standard procedure (3). To probe multiple proteins from the same blot, after electroblotting the nitrocellulose membrane was cut into smaller sections based on the known mobility of the proteins to be assayed.

Affinity purification of L26-eGFP protein. GFP-tagged L26A and L26B proteins were precipitated by following the one-step GFP-Trap_A procedure slightly modified from that suggested in the manufacturer's instructions (Chromotek). Briefly, 50 ml of GFP-tagged or untagged negative-control cells were grown in SD-Leu medium to an OD_{600} of 0.8, harvested, washed with cold water, and concentrated in 500 μl of ice-cold lysis buffer (20 mM Tris-HCl, pH 7.5; 150 mM CH_3COOK; 1.5 mM $MgCl_2$; 1 mM dithiothreitol; 0.2% Triton X-100) containing a protease inhibitor cocktail (Complete; Roche). Cells were disrupted by vigorous shaking with glass beads in a Fastprep-24 (MP Biomedicals) at 4°C, and total cell extracts were obtained by centrifugation in a microcentrifuge at the maximum speed (ca. 16,100 × *g*) for 15 min at 4°C. Each supernatant obtained was mixed with 40 μl of GFP-Trap_A beads, previously equilibrated with the same buffer, and incubated for 2 h at 4°C with end-over-end tube rotation. After incubation, the beads were extensively washed 3 times with 5 ml of the same buffer at 4°C and finally collected. RNA was extracted from the beads and total cell extracts as previously described (4, 20) and then analyzed by Northern blotting as described above.

Antibodies. The following primary antibodies were used: mouse monoclonal antihemagglutinin (anti-HA) 12CA5, mouse monoclonal anti-Myc (Developmental Studies Hybridoma Bank), rabbit polyclonal anti-Has1 (a gift from P. Linder) (28), rabbit polyclonal anti-Nip7 (a gift from D. Goldfarb) (117), rabbit polyclonal anti-Nog1 (a gift from J. Maddock) (32), rabbit polyclonal anti-Nog2 (a gift from M. Fromont-Racine) (90), rabbit polyclonal anti-Nop7 (1), rabbit polyclonal anti-Nsa2 (a gift from M. Fromont-Racine) (57), rabbit polyclonal anti-Rlp24 (a gift from M. Fromont-Racine) (90), rabbit polyclonal anti-Tif6 (a gift from M. Fromont-Racine) (92), mouse monoclonal anti-L3 (a gift from J. R. Warner) (109), rabbit polyclonal anti-L4 (a gift from L. Lindahl), rabbit polyclonal anti-L5 (19), rabbit polyclonal anti-L11 (67), rabbit polyclonal anti-L17 (a gift from S. Rospert) (79), and rabbit polyclonal anti-L25 (a gift from K. Siegers) (36). As secondary antibodies, goat anti-rabbit or anti-mouse horseradish peroxidase-conjugated (Bio-Rad) or alkaline-phosphatase-conjugated (Promega) antibodies were used. TAP-tagged proteins were detected using alkaline phosphatase-conjugated immunoglobulins (Pierce). Immune complexes were revealed with an enhanced chemiluminescence detection kit (Pierce) or using nitroblue tetrazolium (NBT) and 5-bromo-4-chloro-3-indolylphosphate (BCIP) as the substrates (Promega).

Chemical probing *in vivo*. The secondary structure of mature 25S and 5.8S rRNA was assayed by *in vivo* dimethylsulfate (DMS) probing using a protocol adapted from Dutca et al. (26). Briefly, 10 ml of cells was grown in YPD to an OD_{610} of 0.5 and treated with 200 μl of a fresh dilution of DMS (Sigma-Aldrich) in 95% ethanol (1:4, vol/vol) to a final concentration of 50 mM. Treated cells were incubated with shaking at 30°C for 2 min. Reactions were quenched by placing the tubes on ice and adding 5 ml of 0.6 M 2-mercaptoethanol and 5 ml of water-saturated isoamyl alcohol. As a control for the effectiveness of the stop reaction, a control sample was included in which DMS treatment was done after the addition of 2-mercaptoethanol and isoamyl alcohol. Cells were pelleted by centrifugation at 5,000 × *g* for 5 min, and then the liquid phase was carefully removed. Cell pellets were resuspended in 5 ml 0.6 M 2-mercaptoethanol and centrifuged again. Total RNA was immediately extracted from the cells. Nucleotide modifications in the rRNA neighborhood of L26 were assayed by primer extension using oligonucleotides complementary to sequences of the 25S and 5.8S rRNAs in domain I (see Table S3 in the supplemental material). Reverse transcriptase terminated at the base preceding the modified nucleotide. Thus, the modified nucleotides migrated one position higher in the sequencing ladder than in the corresponding DMS lanes.

Computational analysis of ribosome structure. Atomic coordinates of the large r-subunit were retrieved from the Protein Data Bank (PDB; www.rcsb.org) with the accession number 3OFC (25) for *E. coli* and 3U5D and 3U5E (7) for *S. cerevisiae*. The models were visualized with the UCSF

FIG 1 Yeast L26 is the structural homologue of bacterial L24. (A) Localization of L23 (green), L24 (red), and L29 (blue) in the three-dimensional structure of the *E. coli* 50S subunit and of their respective homologues, L25 (green), L26 (red), and L35 (blue), in the three-dimensional structure of the *S. cerevisiae* 60S subunit. The cartoons were generated with the UCSF Chimera program, using the atomic model for the crystal structure of the *E. coli* 70S ribosome (PDB file 3OFC [25]) and the yeast 80S ribosome (PDB files 3U5D and 3U5E [7]). (B) Close-up view of the position of *E. coli* L24 (left) and yeast L26 (right) in the context of their binding sites in the respective large subunits. Only rRNA residues situated at or closer than 12 Å from L24 or L26 are shown (bases and phosphate backbone). Base numbering follows the 23S rRNA sequence deposited for the *E. coli* 50S r-subunit (PDB file 3OFC [25]) and the 25S and 5.8S rRNA sequences deposited for the yeast 60S r-subunit (PDB file 3U5D [7]), respectively. Selected residues are labeled in black (23S and 25S rRNAs) or in blue (5.8S rRNA). (C) Secondary structure of domains I from *E. coli* 23S rRNA and *S. cerevisiae* 25S/5.8S rRNAs. The structures were taken from The Comparative RNA Web Site (http://www.rna.icmb.utexas.edu/) (11). Yeast 5.8S rRNA sequence is highlighted in yellow. Red circles indicate rRNA residues situated closer than 5 Å from *E. coli* L24 or yeast L26 proteins.

Chimera program (www.cgl.ucsf.edu/chimera) (76). Secondary structures of rRNAs from *E. coli* and *S. cerevisiae* were taken from The Comparative RNA Web Site (http://www.rna.icmb.utexas.edu/) (11).

RESULTS

L26 is an evolutionarily conserved r-protein. Yeast r-protein L26 is encoded by two paralogous genes (*RPL26A* and *RPL26B*), a feature that is characteristic of most yeast r-protein genes (111). These genes produce two small basic r-proteins of 127 amino acids, L26A and L26B. The r-proteins are nearly identical, differing only at position 26, glutamine in L26A and glutamic acid in L26B (*Saccharomyces* Genome Database [www.yeastgenome.org]). L26 is highly conserved between species, sharing notable sequence identity with archaeal and eubacterial L24 (Ribosomal Protein Gene Database [http://ribosome.med.miyazaki-u.ac.jp/]; also see Fig. S2 in the supplemental material). Moreover, prokaryotic L24 and eukaryotic L26 are RNA binding proteins that occupy similar locations in the large r-subunit. Yeast L26 is located near L35 and L25 in close proximity to the polypeptide exit tunnel; the three proteins are clearly arranged in a manner identical to their bacterial counterparts (Fig. 1A). Most importantly, prokaryotic L24 and eukaryotic L26 r-proteins specifically recognize the same structurally conserved region in domain I of bacterial 23S rRNA and eukaryotic 25S/5.8S rRNAs, respectively (Fig. 1B and C). Thus, it can be concluded that bacterial L24 and eukaryotic L26 are unequivocal functional orthologues.

Yeast L26 assembles in the nucle(ol)us within early preribosomal particles. Assembly of r-subunits occurs mainly in the nucle(ol)us, although a few 60S r-proteins appear to stably load only with cytoplasmic pre-60S r-particles, such as L24 (54, 90), or preferentially with them, such as L10 or P0 (48, 60, 84, 112). Pulse-chase studies have suggested that yeast L26 can assemble at an early nuclear stage of the 60S r-subunit maturation process (54); however, the L26 primary sequence seems to lack a potential nuclear localization signal (NLS) (according to the cNLS mapper program [50]). To explore in which cellular compartment L26 assembles, we monitored the localization of a functional L26A-eGFP construct upon induction of the dominant-negative *NMD3Δ100* allele (6). Nmd3 is the Crm1-dependent adapter for the export of preribosomal particles through nuclear pores (43). The dominant-negative Nmd3Δ100 protein traps pre-60S r-particles in the nucle(ol)us (43). As shown in Fig. 2, the L26A-eGFP construct accumulates in the nucleus for most of the cells examined upon overexpression of the Nmd3Δ100 protein but is found in the cytoplasm under noninducible conditions. No change in the cytoplasmic distribution of L26A-eGFP was observed upon overexpression of the wild-type Nmd3 protein (data not shown). Similar results were obtained when the L25-eGFP reporter was used, which has been clearly described to assemble in the nucle(ol)us (for examples, see references 4, 43, and 44).

To investigate in more detail the timing of assembly of L26, we affinity purified L26B-eGFP-containing complexes using GFP-Trap beads (see Materials and Methods) and determined which pre-rRNA intermediates copurified by Northern blotting. As shown in Fig. 3, and as expected for a 60S r-protein, there was significant copurification of mature 25S, 5.8S, and 5S rRNAs with L26B-eGFP. Moreover, mature 18S rRNA was also efficiently copurified with L26B-GFP. As previously described (4), we believe that this must reflect the common nonspecific association of 40S with 60S r-subunits in 80S couples in Mg^{2+}-containing buffers or

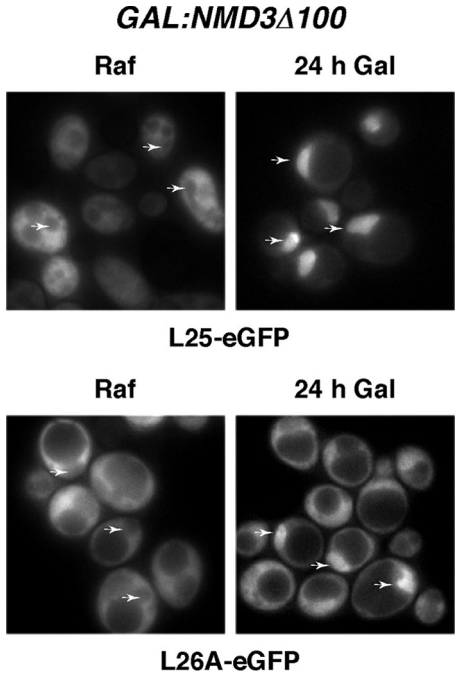

FIG 2 L26 assembles within the nucle(ol)us. Localization of L25-eGFP and L26A-eGFP upon induction of an *NMD3* dominant-negative allele; *rpl26* null cells expressing L25-eGFP or L26A-eGFP were transformed with the pRS316-*GAL-NMD3Δ100* plasmid, and transformants were grown in the presence of raffinose (SRaf-Leu-Ura). Galactose was then added to fully induce the Nmd3Δ100 protein. The GFP signal was inspected by fluorescence microscopy after 24 h. Arrows point to nuclear fluorescence.

ribosomes engaged in translation. Interestingly, 27S and 7S pre-rRNAs were also detected (Fig. 3). In clear contrast, practically background levels were detected for 35S and 20S pre-rRNAs. All of these results are specific, since no RNAs were detected upon affinity purification from extracts of the untagged strain. Similar results were obtained when L26A-eGFP was used as the bait (data not shown). Taken together, these data strongly suggest that L26 stably assembles into early nucle(ol)ar pre-60S r-particles, although it might interact weakly with 90S preribosomal particles.

Yeast L26 is completely dispensable for growth. To study the role of yeast L26 in ribosome biogenesis and function, we first analyzed the phenotypic consequences of deleting either the *RPL26A* or *RPL26B* gene. As shown in Fig. 4A, *rpl26aΔ* and *rpl26bΔ* single mutants grow identically to the wild-type strain at different temperatures (16, 30, and 37°C) on YPD plates. Moreover, no significant differences were found when doubling times were calculated for cultures grown in liquid YPD or SD medium at any of the temperatures mentioned above (data not shown). To test whether L26 is required for growth, *rpl26aΔ* and *rpl26bΔ* haploid strains were mated and the resulting diploids sporulated. Most of the tetrads yielded four viable spores. Recombinant ditypes were obtained, suggesting that cells could grow without any L26. The absence of both *RPL26A* and *RPL26B* was verified by PCR (data not shown). A double disruptant for *RPL26A* and *RPL26B* (here named the *rpl26* null strain) grew apparently as well as the wild-type strain on solid or in liquid media (Fig. 4A and data not shown). Moreover, a *GAL*::*HA-RPL26A rpl26bΔ* strain (here named the *GAL*::*RPL26* strain) grew identically in YPGal and YPD (see Fig. S3 in the supplemental material). To further ascertain the

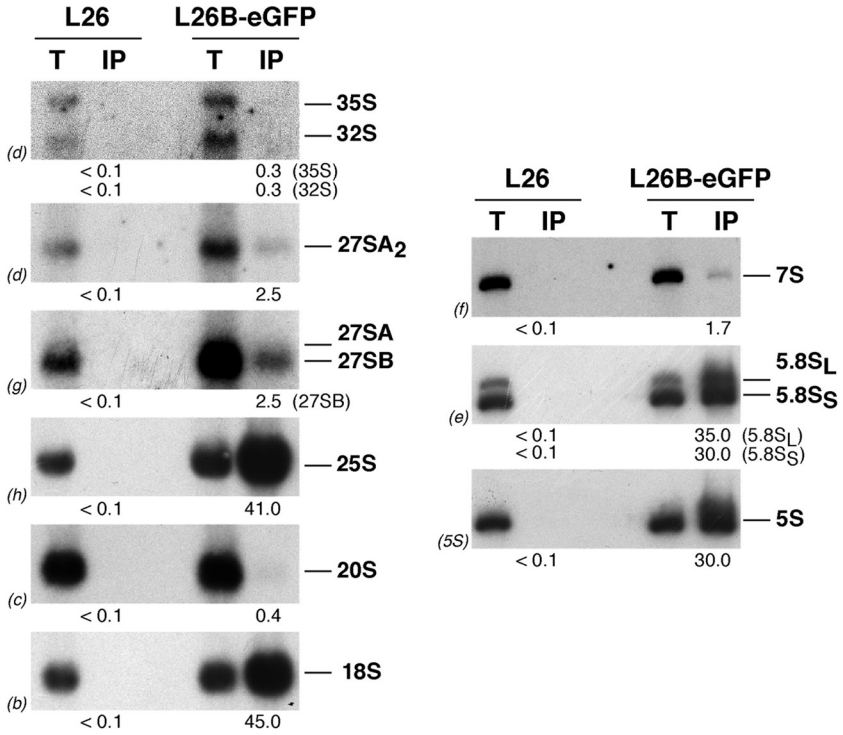

FIG 3 L26-GFP associates with pre-60S ribosomal particles. GFP-tagged L26 was affinity purified with GFP-Trap_A beads from total cellular extracts of *rpl26* null cells expressing L26B-eGFP. Wild-type cells were used as an untagged L26 control. RNA was extracted from the pellets obtained after purification (lanes IP) or from an amount of total extracts corresponding to 1/100 of that used for purification (lanes T) and was subjected to Northern analysis of pre- and mature rRNAs. Probes (in parentheses) are described in Fig. S1A and Table S3 in the supplemental material. Signal intensity was measured by phosphorimager scanning; values (below each IP lane) refer to the percentage of each RNA recovered after purification.

loss of *RPL26* expression in the *rpl26* null strain, production of *RPL26* transcripts was examined by Northern blotting using a probe common to the *RPL26A* and *RPL26B* genes. As shown in Fig. 4B, no specific *RPL26* transcript could be detected in *rpl26* null cells. Interestingly, the analysis of single *rpl26a*Δ and *rpl26b*Δ strains suggests that the *RPL26B* gene contributes more to *RPL26* mRNA levels than *RPL26A*. Altogether, our results clearly demonstrate that L26 is completely dispensable for cell growth under standard laboratory conditions. This finding is independent of the yeast genetic background and clearly not the consequence of the appearance of spontaneous extragenic suppressors (data not shown).

The absence of L26 leads to very mild defects in ribosome biogenesis. Thus far, most studied r-proteins contribute to different steps of ribosome biogenesis (for examples, see references 4, 29, and 78 and references therein). To study the role of yeast L26 in ribosome biogenesis, we first analyzed polysome profiles from cell extracts of the different *rpl26* deletion strains and compared them to that from an isogenic wild-type counterpart. As shown in Fig. 5, the *rpl26a*Δ and *rpl26b*Δ single mutants and the *rpl26* null strain showed a very minor deficit in 60S r-subunits, as judged from the slight reduction of the levels of free 60S relative to 40S r-subunits and the appearance of modest half-mer polysomes. Identical results were obtained upon depletion of L26 in the *GAL*::*RPL26* strain (see Fig. S4 in the supplemental material).

To clarify whether L26 is required for pre-rRNA processing, we studied the kinetics of rRNA production by [5,6-^{3}H]uracil pulse-chase analysis with the *rpl26* null strain and its isogenic wild-type counterpart. Both strains displayed very similar kinetics of rRNA synthesis (Fig. 6). However, we could clearly observe a moderate delay in both 35S and 27SB pre-rRNA processing for the *rpl26* null mutant with practically no evident consequences in the final production of both the mature 25S and 5.8S rRNA. Thus, the minor deficit in 60S r-subunits in the strain lacking L26 might be the consequence of a slight delay in 27SB pre-rRNA processing.

Steady-state levels of pre- and mature rRNAs were analyzed by Northern hybridization and primer extension. Consistent with the previous data, only mild effects were observed in pre-rRNA processing, especially for the *rpl26a*Δ and *rpl26* null strains (Fig. 7). In these mutants, there was a slight accumulation of both 35S and 23S pre-rRNAs. The 23S species results from 35S pre-rRNA cleavage at site A_3 without prior cleavage at sites A_0, A_1, and A_2 (108). A modest accumulation of $27SA_2$ and 27SB pre-rRNAs was also detected. As a consequence, a very slight decrease in the levels of mature 25S was found (Fig. 7A; also see Table S4 in the supplemental material). Analysis of low-molecular-mass RNA species showed that levels of 7S pre-rRNAs and mature 5S and 5.8S rRNAs remained unaffected (Fig. 7B). Primer extension analyses demonstrated that the levels of $27SA_2$, $27SA_3$, $27SB_L$, and $27SB_S$ pre-rRNAs modestly increased in the *rpl26* null strain (Fig. 7C). Similar primer extension results were obtained upon the depletion of L26 (see Fig. S5 in the supplemental material). We conclude that L26 is not essential for the maturation of rRNAs. Instead, L26 seems to be needed to optimize all of the 27S pre-rRNA processing reactions. The absence of L26 also slightly delays processing at the early cleavage sites A_0 to A_2, as similarly occurs for many mutants

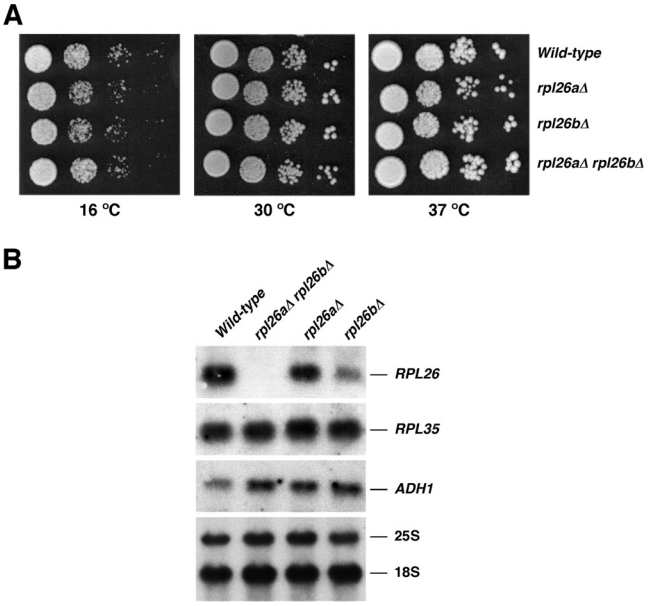

FIG 4 L26 is not essential for growth. (A) The strains BY4741 (wild type), RBY272, a deletant of *RPL26A* (*rpl26a*Δ), RBY274, a deletant of *RPL26B* (*rpl26b*Δ), and RBY276, an *rpl26* null strain (*rpl26a*Δ *rpl26b*Δ), were grown in liquid YPD and diluted to an OD_{600} of 0.05. Serial dilutions were spotted onto YPD plates. Plates were incubated at 30 and 37°C for 3 days or at 16°C for 6 days. (B) Total RNA was extracted from cell extract of the strains, separated by gel electrophoresis, transferred to a nylon membrane, and subjected to Northern analysis. The same filter was consecutively hybridized with α-^{32}P-DNA probes specific for *RPL26*, *RPL35*, and *ADH1* mRNAs. Mature 25S and 18S rRNAs, which were used as markers to check equal loading, were probed with γ-^{32}P-labeled oligonucleotides (see Fig. S1A and Table S3 in the supplemental material).

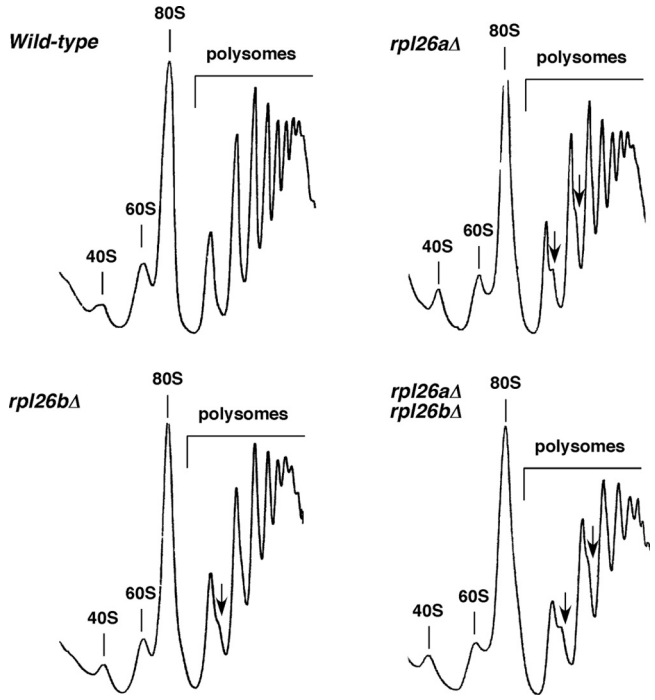

FIG 5 Absence of L26 results in a very slight deficit of 60S r-subunits. Polysome profiles are shown for the wild-type and the L26-deficient strains described in Fig. 4. Cells were grown in YPD at 30°C and harvested at an OD_{600} of around 0.8. Total extracts were prepared, and 10 A_{260} units of each one were resolved on 7 to 50% sucrose gradients. The A_{254} was continuously monitored. Sedimentation is from left to right. The peaks of free 40S and 60S r-subunits, 80S free couples/monosomes, and polysomes are indicated. Half-mer polysomes are labeled by arrows.

in genes encoding 60S r-subunit synthesis factors and 60S r-proteins. This is likely due to inefficient recycling of *trans*-acting factors that cannot efficiently dissociate from aberrant pre-60S r-particles (for further discussion, see references 33, 85, and 108).

The composition of pre-60S ribosomal particles lacking L26 is not significantly affected. To explore the pre-60S ribosomal particles from an L26-deficient strain, we affinity purified Nop7-TAP complexes from *GAL*::*RPL26* cells before or after depletion of L26. We then analyzed the protein constituents of the purified complexes by SDS-PAGE and Western blotting. Nop7-TAP complexes are a mixture of early, intermediate, and late nuclear pre-60S assembly intermediates (39, 71). The SDS-PAGE profiles of purified pre-60S r-particles from cells depleted of L26 were remarkably similar to those from cells expressing L26. No changes were observed in the levels of the set of r-proteins and most r-subunit assembly factors evaluated by Western blotting (Fig. 8). However, consistent with the slight delay in processing of late 27S intermediates observed in an *rpl26* null mutant, levels of late-assembling factors Nsa2 and Nog2/Nug2, which are required for ITS2 processing (57, 89), were modestly diminished upon L26 depletion. Thus, the composition of pre-60S r-particles lacking L26 is not significantly altered.

Nuclear export of pre-60S r-particles is minimally impaired in the absence of L26 ribosomal protein. To further characterize the consequences of the absence of L26 on ribosome biogenesis, we determined whether the *rpl26* null mutant was impaired in nuclear export of pre-60S r-particles. To do this, we analyzed the location of the 60S r-subunit reporter L25-eGFP (34) in this mutant and the isogenic wild-type strain. As shown in Fig. 9, L25-eGFP was, as expected for an r-protein, excluded from the vacuole and found predominantly in the cytoplasm in the wild-type strain. However, we observed a faint nuclear retention of the fluorescence signal of the L25-eGFP reporter in about half of the *rpl26* null cells examined. In most cells, the fluorescence signal was restricted to the nucleolus, which was detected with the nucleolar marker mRFP-Nop1 (34). No accumulation of nuclear fluorescence was observed when we studied the localization of the 40S r-subunit reporter S3-eGFP (64) in either the wild type or the *rpl26* null mutant (Fig. 9). We conclude that mild defects of both intranuclear and nucleocytoplasmic transport become evident when L26 r-protein does not assemble into pre-60S r-particles. These defects are apparently specific, as transport of pre-40S r-particles is unaffected in the absence of L26. Impaired export of preribosomal particles has been reported in strains mutant for genes encoding r-proteins and r-subunit biogenesis proteins that are not bona fide export factors or adaptors. In such cases, this defect supposedly arises from activation of a nuclear surveillance system that prevents export of these particles when they are aberrant or misassembled (discussed in reference 102). Thus, pre-60S r-particles lacking L26 might be substrates of these nuclear retention systems even though we could not detect significant alterations in their composition.

L26 has a minor role in ribosome structure and function. To evaluate changes in the global composition of mature ribosomes

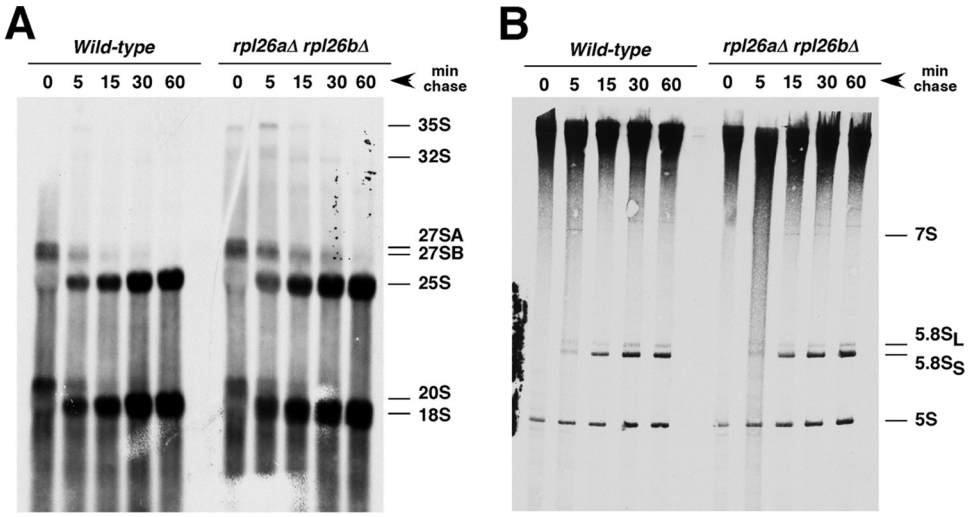

FIG 6 Absence of L26 slightly delays processing of 27SB pre-rRNAs. Wild-type and *rpl26* null strains were transformed with the *CEN URA3* YCplac33 plasmid and then grown at 30°C in SD-Ura to an OD_{600} of around 0.8. Cells were pulse-labeled for 2 min with [5,6-^{3}H]uracil and then chased for 5, 15, 30, and 60 min with an excess of unlabeled uracil. Total RNA was extracted, and samples (20,000 cpm per sample) were loaded and separated on a 1.2% agarose–6% formaldehyde gel (A) or a 7% polyacrylamide–8 M urea gel (B), transferred to nylon membranes, and visualized by fluorography. The positions of the different pre-rRNAs and mature rRNAs are indicated.

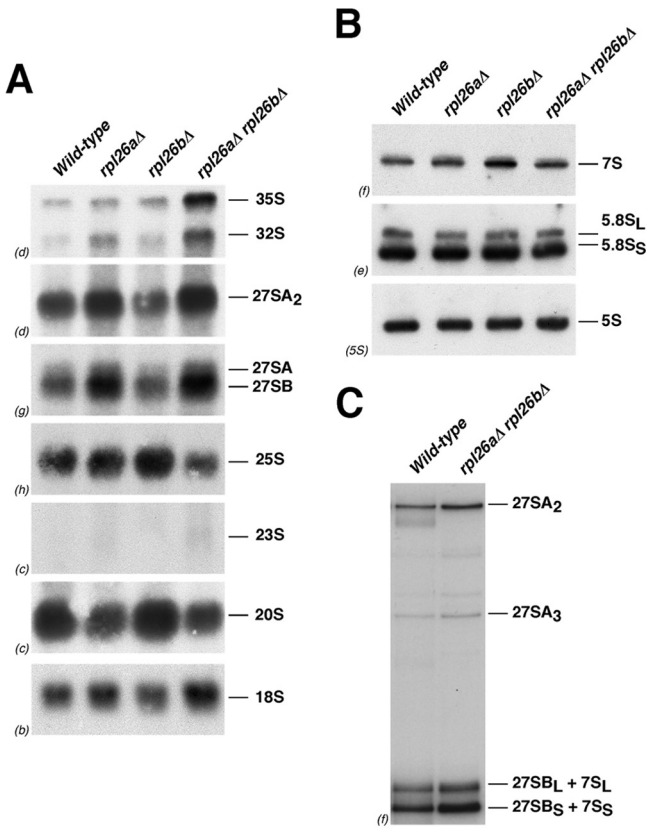

FIG 7 Absence of L26 slightly alters pre-rRNA processing. The wild-type and L26-deficient strains described in the legend to Fig. 4 were grown in YPD at 30°C and harvested at an OD_{600} of around 0.8. Total RNA was extracted and subjected to Northern hybridization or primer extension. Probes (in parentheses) are described in Fig. S1A and Table S3 in the supplemental material. (A) Northern analysis of high-molecular-mass pre- and mature rRNAs. (B) Northern analysis of low-molecular-mass pre- and mature rRNAs. (C) Primer extension analysis of 27S pre-rRNAs. Probe f within ITS2 was used.

from the L26-deficient strain, we first enriched ribosomes from wild-type and *rpl26* null cells by a standard fractionation protocol. r-proteins then were separated by SDS-PAGE and analyzed by Western blotting. As shown in Fig. S6 in the supplemental material, ribosomes from wild-type and *rpl26* null cells were clearly similar. We next addressed the effect of the loss of L26 on its binding site and the adjacent rRNA neighborhood in 60S r-subunits. To do so, wild-type and *rpl26* null cells were treated with the RNA methylating agent DMS, which preferentially methylates adenines and cytosines unless they are protected by the formation of base pairs, ternary structure, or protein binding (114). Guanosines and uracils are also methylated by DMS *in vivo*, albeit rarely (66). Methylation was detected as strong stops in primer extension reactions (see Materials and Methods). L26 interacts with numerous sites in domain I of 25S/5.8S rRNA (Fig. 1B and C) (7). DMS probing reveals that several nucleotides corresponding or in close proximity to the binding region of L26 become differentially modified in its absence (Fig. 10; also see Fig. S7 in the supplemental material). As expected, a majority of these sites become more accessible when L26 is missing. Interestingly, a few unpaired nucleotides show decreased accessibility in 60S r-subunits lacking L26 (Fig. 10; also see Fig. S7). These results suggest that the absence of L26 leads to clear rRNA conformational changes, but these are not sufficient to induce the destabilization and loss of other r-proteins in 60S r-subunits.

To determine whether these structural differences affect the function of L26-deficient ribosomes, we monitored various aspects of translation *in vivo*. First, we measured the hypersensitivity or resistance to different protein translation inhibitors, which have been described as convenient probes for changes in ribosome function (115). Second, we tested the maintenance of the killer virus system, which is highly sensitive to changes in the concentration of free 60S r-subunits (74). Third, we evaluated translational accuracy by quantitatively monitoring changes in −1 and +1 PRF, the readthrough of nonsense codons, and the stringency of start codon selection (23, 59, 104). Surprisingly, the absence of

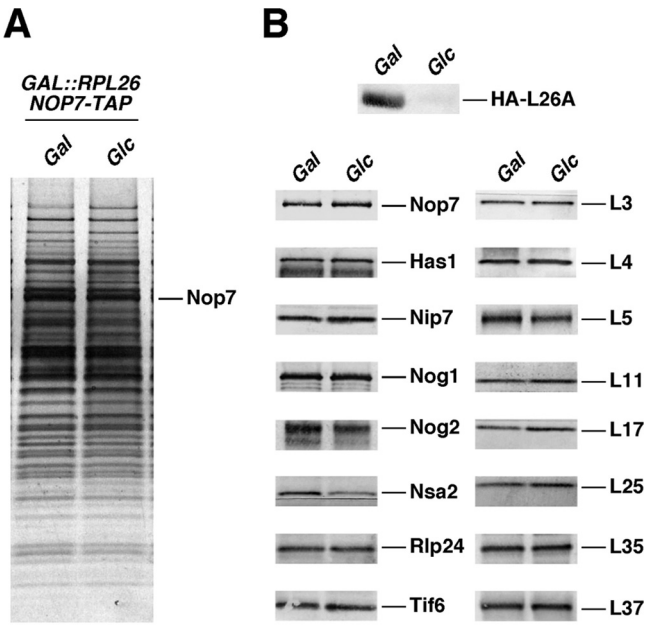

FIG 8 Depletion of L26 does not significantly affect composition of pre-60S ribosomal particles. (A) TAP-tagged Nop7 was used to purify nuclear pre-60S particles from a conditional *GAL::RPL26* strain (JWY9634; *GAL::HA-RPL26A rpl26bΔ NOP7-TAP*) grown in YPGal (Gal) or shifted to YPD (Glc). Copurifying proteins were separated by SDS-PAGE and stained with silver. (B) Western blotting was used to specifically assay the presence of selected ribosome assembly factors and ribosomal proteins in Nop7-TAP-containing preribosomal particles before and after depletion of L26.

L26 does not result in changes in 60S r-subunits that significantly impact these translation properties (summarized in Table S5 in the supplemental material).

DISCUSSION

In this work, we have addressed the role of the evolutionarily conserved r-protein L26 in yeast 60S r-subunit biogenesis, structure, and function. L26 and its bacterial paralogue L24 map onto equivalent positions surrounding the nascent polypeptide exit tunnel in both eukaryotic and prokaryotic large r-subunits, respectively.

Analysis of an *rpl26* null mutant shows that L26 is entirely dispensable for cell growth at different temperatures under standard laboratory conditions. Similar results have been recently reported by Steffen and coworkers (97). Ten other 60S r-subunit proteins have been described as not being essential in yeast (5, 8, 15, 24, 35, 75, 78, 80, 86, 96, 97, 116). The absence of some of these nonessential r-proteins reduces cell growth rates to different extents; for example, either L38 (96) or L41 (116) is almost dispensable for growth, while L12 is practically essential (8).

Here, we have addressed the role of L26 r-protein in ribosome biogenesis. The dispensability of L26 denotes that almost wild-type ribosomes are being assembled in an L26-deficient strain under standard laboratory conditions. Hence, polysome profile, pulse-chase, Northern blot, primer extension, and preribosomal compositional analysis clearly indicate that the contribution of L26 to ribosome biogenesis is very minor. In the absence of L26, we could observe only a modest deficit of 60S r-subunits. This is most likely due to delayed 27SB pre-rRNA processing, which might be brought about by moderately reduced levels of assembly factors required for efficient processing of 27SB pre-rRNAs (i.e., Nsa2 and Nog2) in pre-60S r-particles lacking L26. Consequently, the relative amounts of 27S pre-rRNAs slightly increase, although both the kinetics and the steady-state levels of 7S pre-rRNAs remain unaffected. The deficiency of L26 also leads to a mild delay in pre-rRNA processing at the early cleavage sites A_0, A_1, and A_2 without consequences in the levels of 20S pre-rRNA and mature 18S rRNA.

We have analyzed the structure of L26-deficient and wild-type ribosomes by DMS probing experiments. Our results indicate that the absence of L26 induces significant changes in the conformation of 25S/5.8S rRNA domain I. As expected, L26-deficient ribosomes showed increased nucleotide modification relative to wild-

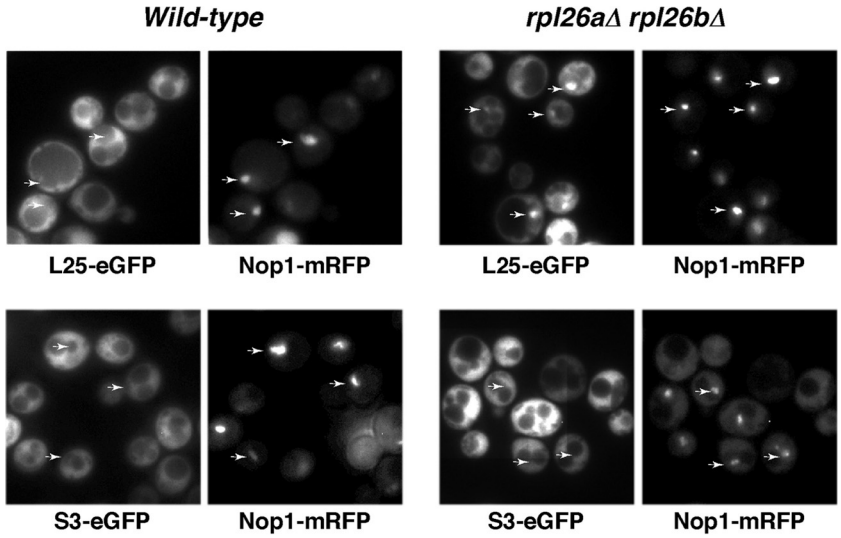

FIG 9 Absence of L26 leads to some nuclear retention of the 60S r-subunit reporter L25-eGFP. Strains BY4741 (wild type) and RBY276 (*rpl26aΔ rpl26bΔ*) were transformed with plasmids that expressed Nop1-mRFP and either L25-eGFP or S3-eGFP from their cognate promoters. Cells were grown at 30°C in SD-Ura. The subcellular localization of the GFP-tagged ribosomal proteins and the Nop1-mRFP nucleolar marker were analyzed by fluorescence microscopy. Arrows point to nucleolar fluorescence.

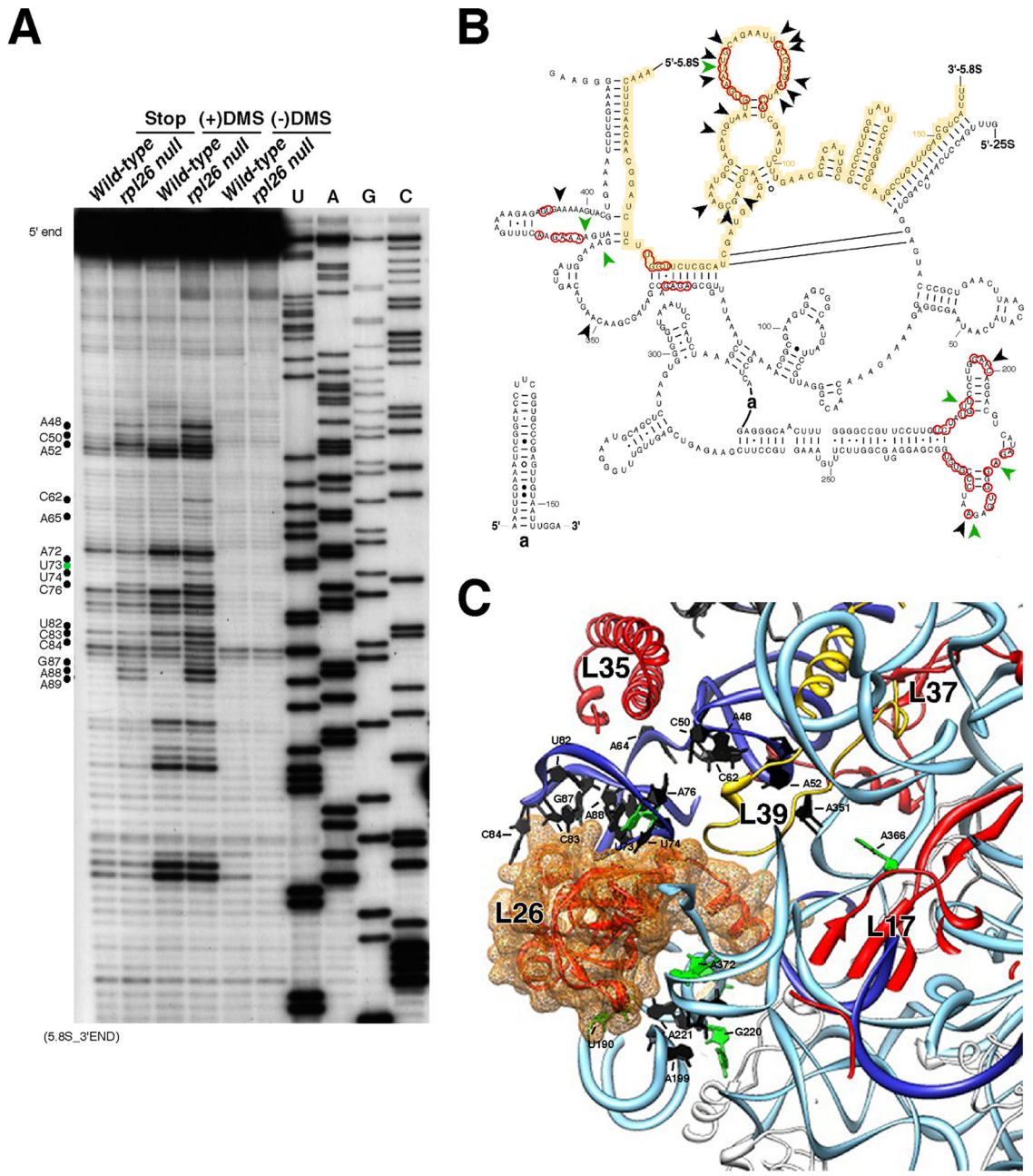

FIG 10 Absence of L26 induces changes in the structure of 25S/5.8S rRNA domain I. (A) *In vivo* DMS chemical probing experiment of the rRNA structure around the binding site of L26. Wild-type and *rpl26* null cells were treated with DMS. Total RNA was extracted from unmodified (−DMS) and modified (+DMS) yeast cells and analyzed by primer extension using the 5.8S_3′END primer (see Table S3 in the supplemental material). U, A, G, and C represent dideoxy sequencing lanes done with the same primer. Stop controls indicate the efficiency of quenching reactions after DMS treatment. Black and green dots denote nucleotides with stronger and weaker reactivity to DMS in the *rpl26* null strain, respectively. (B) Secondary structure of yeast 25S/5.8S rRNA domain I (the legend to Fig. 1 provides further details). Red circles indicate nucleotides situated closer than 5 Å from the yeast L26 protein. Nucleotides with stronger and weaker reactivity to DMS in the *rpl26* null strain are labeled with black or green arrowheads, respectively (see Fig. S7 in the supplemental material for full DMS probing gels). (C) Close-up view of the three-dimensional arrangement of the yeast 25S/5.8S rRNA domain I, including the ribosomal proteins L17, L35, and L37 (red); L26 (red; the surface is also shown); and L39 (yellow). Only the base side chains of the nucleotides undergoing changes in the DMS reactivity are highlighted and labeled in black or green, as described above. Note that the structure is clipped to simplify the figure.

type ones in regions at or near the binding site of L26. Some rRNA residues bound by adjacent r-proteins in mature ribosomes also became more accessible to DMS. This is most likely not due to the mere absence of these r-proteins, since L26-deficient ribosomes remain otherwise intact relative to the wild type. Furthermore, we also observed that a few nucleotides that do not participate in base pairing showed decreased DMS modification in the absence of L26, suggesting that these nucleotides are now involved in base pairing or are protected by an r-protein in close proximity. We conclude that the absence of assembly of L26 slightly affects the

conformation of yeast rRNA domain I without significant effects on the binding of its neighboring r-proteins. However, we cannot exclude the possibility that the arrangement of these r-proteins relative to rRNA (e.g., L39) (Fig. 10C) is modestly altered.

To monitor the function of L26 in translation, we performed different *in vivo* assays in the L26-deficient strain. None of the assays provided positive results, indicating that L26-deficient ribosomes have no appreciable alterations in either the kinetics or fidelity of protein synthesis. Given the location of L26 near the polypeptide exit tunnel, it is noteworthy that the absence of L26 does not promote hypersensitivity to AZC, a common feature of ribosome-associated chaperone mutants (2). Ribosome-associated chaperones assist in the folding of the nascent polypeptide chains by docking on selected r-proteins at the tunnel exit site (reviewed in reference 51). Thus, our results strongly suggest that ribosome-associated chaperones still interact optimally with L26-deficient ribosomes.

We have also addressed the course of assembly of L26. Seminal work done in yeast and HeLa cells suggested that L26 assembles in the nucleus (54, 55). Here, we show that functional GFP-tagged L26 proteins accumulate in the nucleus upon inhibition of nucleocytoplasmic export of pre-60S r-particles by overexpression of the dominant-negative Nmd3Δ100 protein. In agreement with this, analysis of pre-rRNA species associated with L26-eGFP indicates that L26 is stably assembled into the earliest pre-60S ribosomal particles. It has been reported that L26, together with L17, L35, and L37, fails to assemble upon depletion of factors (Erb1, Nop7, Nop15, Nsa3/Cic1, Rlp7, Rrp1, and Ytm1) (87) and r-proteins (L7 and L8) (45) affecting $27SA_3$ pre-rRNA processing. Interestingly, the L17, L26, L35, and L37 r-proteins are adjacent to each other in mature 60S r-subunits and associated mostly with domain I of 25S/5.8S rRNAs (7). Strikingly, the loss of function of the A_3 factors and L17, L35, and L37 r-proteins causes a complete block in 27S pre-rRNA processing, which is not comparable to the slight 27S pre-rRNA processing delay observed in the absence of L26 (4, 45, 78, 87; M. Gamalinda, unpublished results). We and others believe that stable assembly of L17, L26, L35, and L37 r-proteins requires a proper rRNA conformation established by the A_3 factors and r-proteins L7 and L8 (38, 45, 87). Analysis of Nop7-TAP complexes upon depletion of L26 clearly indicates that L26 is not required for the association of distinct early or late assembly factors or the proper assembly of r-proteins bound to 5.8S/25S rRNA domain I, including L17, L35, and L37. This scenario is different from that of bacterial assembly, where L24 seems to be critical to structure 23S rRNA domain I. *E. coli* L24, together with L3, are the only r-proteins able to initiate the assembly of 50S r-subunit *in vitro* (69, 93). Consistent with this, experimental evidence strongly suggests that L24 is also one of the earliest r-proteins to assemble *in vivo* (17, 27, 77; discussed in references 49 and 93). Moreover, recruitment *in vitro* of both L22 and L29, the respective bacterial homologues of yeast L17 and L35, depends on prior binding of L24 (discussed in reference 49).

Why is yeast L26 dispensable for growth? The obvious answer is that yeast L26 does not play an important role in ribosome assembly, structure, and/or function. Interestingly, L26 is also not essential in *Schizosaccharomyces pombe* (according to Pombase [http://www.pombase.org/] and J. de la Cruz, unpublished results). However, reports in flybase (http://flybase.org) and wormbase (http://wormbase.org) indicate that the lack of function of L26 is lethal in *Drosophila* and *Caenorhabditis*, respectively, although effects on ribosome production or function remain untested. For mammalian cells, the literature is unclear. While Robledo et al. showed that depletion of L26 might be deleterious since it impairs r-subunit maturation (82), Takagi et al. described that depletion of L26 neither altered overall translation nor perturbed ribosome synthesis (100). An extraribosomal role for the human L26 r-protein has also been reported; human L26 can bind to the 5′ untranslated region of p53 mRNA to stimulate its translation (100). Human L26 can also posttranslationally modulate the levels of p53 by blocking the E3 ubiquitin ligase activity of the HDM2 protein, which is responsible for maintaining low levels of p53 in unstressed cells (73, 118). Clearly, the contribution to cell growth of the ribosomal versus the extraribosomal function of L26 in metazoans must be addressed. *E. coli* L24 is essential for growth only at high temperatures, although the mutant lacking L24 exhibits a low growth rate even at permissive temperatures (10, 14, 42, 94). The growth defect of the bacterial mutant lacking L24 seems to be due solely to underproduction of large r-subunits as a consequence of impaired assembly (42). Indeed, it has been demonstrated that L24 is not important for ribosome function *in vitro* (42, 95), as is apparently the case for yeast L26 *in vivo*.

In conclusion, this work underscores interesting differences in the assembly of bacterial L24 and yeast L26 r-proteins. While not essential for assembly under normal growth conditions in either organism, the absence of L24 has a greater effect on *E. coli* than the absence of L26 in yeast. We have initiated experiments to uncover the dispensability of yeast L26. We are exploring diverse functional assays, including different stresses and limitation of nutrients, to find conditions where the *rpl26* null mutant shows reduced fitness compared to the wild type. Moreover, we are performing synthetic-lethal analyses to find assembly factors or r-proteins needed to ensure optimal 60S r-subunit assembly in L26-deficient cells. Our preliminary results suggest that yeast L37, which is not conserved in bacterial ribosomes (58), is important to maintain the stability of L26-deficient ribosomes; thus, the growth of an *rpl37a*Δ *rpl26a*Δ *rpl26b*Δ triple mutant strain is substantially poorer than the growth of the *rpl37a*Δ strain, especially at low temperatures (22 and 16°C). Further studies are clearly required to understand the cellular role of L26 r-protein.

ACKNOWLEDGMENTS

We are grateful to all colleagues mentioned in the text for their gifts of material used in this study. We are indebted to A. Díaz-Quintana for his invaluable help with the analysis of the molecular structure of yeast L26 and related data. We also thank A. Fernández-Pevida for help during the *in vivo* translational assays, M. Carballo, L. Navarro, and C. Reyes of the Biology Service (CITIUS) from the University of Seville for help with the phosphorimager analysis, J. Talkish for advice about *in vivo* chemical probing, and J. Jakovljevic for critical reading of the manuscript.

This work was supported by grants from the National Science Foundation (MCB 0818534) to J. L.W. and the Spanish Ministry of Science and Innovation and ERDF (BFU2010-15690) and the Andalusian Government (CVI-271, P07-CVI-02623 and P08-CVI-03508) to J.C. R.B. is a recipient of an FPI fellowship from the Andalusian Government.

REFERENCES

1. **Adams CC, et al.** 2002. *Saccharomyces cerevisiae* nucleolar protein Nop7p is necessary for biogenesis of 60S ribosomal subunits. RNA **8**:150–165.
2. **Albanèse V, Yam AY, Baughman J, Parnot C, Frydman J.** 2006. Systems analyses reveal two chaperone networks with distinct functions in eukaryotic cells. Cell **124**:75–88.

3. **Ausubel FM, et al.** 1994. *Saccharomyces cerevisiae*, p 13.0.1–13.14.17. Current protocols in molecular biology, vol 2. John Wiley & Sons, Inc., New York, NY.
4. **Babiano R, de la Cruz J.** 2010. Ribosomal protein L35 is required for 27SB pre-rRNA processing in *Saccharomyces cerevisiae*. Nucleic Acids Res. **38**:5177–5192.
5. **Baronas-Lowell DM, Warner JR.** 1990. Ribosomal protein L30 is dispensable in the yeast *Saccharomyces cerevisiae*. Mol. Cell. Biol. **10**:5235–5243.
6. **Belk JP, He F, Jacobson A.** 1999. Overexpression of truncated Nmd3p inhibits protein synthesis in yeast. RNA **5**:1055–1070.
7. **Ben-Shem A, et al.** 2011. The structure of the eukaryotic ribosome at 3.0 Å resolution. Science **334**:1524–1529.
8. **Briones E, Briones C, Remacha M, Ballesta JPG.** 1998. The GTPase center protein L12 is required for correct ribosomal stalk assembly but not for *Saccharomyces cerevisiae* viability. J. Biol. Chem. **273**:31956–31961.
9. **Bubunenko M, et al.** 2006. 30S ribosomal subunits can be assembled *in vivo* without primary binding ribosomal protein S15. RNA **12**:1229–1239.
10. **Cabezón T, Herzog A, Petre J, Yaguchi M, Bollen A.** 1977. Ribosomal assembly deficiency in an *Escherichia coli* thermosensitive mutant having an altered L24 ribosomal protein. J. Mol. Biol. **116**:361–374.
11. **Cannone JJ, et al.** 2002. The comparative RNA web (CRW) site: an online database of comparative sequence and structure information for ribosomal, intron, and other RNAs. BMC Bioinformatics **3**:2. doi: 10.1186/1471-2105-3-2.
12. **Cigan AM, Pabich EK, Donahue TF.** 1988. Mutational analysis of the *HIS4* translational initiator region in *Saccharomyces cerevisiae*. Mol. Cell. Biol. **8**:2964–2975.
13. **Connolly K, Culver G.** 2009. Deconstructing ribosome construction. Trends Biochem. Sci. **34**:256–263.
14. **Dabbs ER.** 1982. A spontaneous mutant of *Escherichia coli* with protein L24 lacking from the ribosome. Mol. Gen. Genet. **187**:453–458.
15. **DeLabre ML, Kessl J, Karamanou S, Trumpower BL.** 2002. RPL29 codes for a non-essential protein of the 60S ribosomal subunit in *Saccharomyces cerevisiae* and exhibits synthetic lethality with mutations in genes for proteins required for subunit coupling. Biochim. Biophys. Acta **1574**:255–261.
16. **de la Cruz J, Kressler D, Linder P.** 2004. Ribosomal subunit assembly, p 258–285. *In* Olson MOJ (ed), The nucleolus. Landes Bioscience, Austin, TX.
17. **de Narvaez CC, Schaup HW.** 1979. *In vivo* transcriptionally coupled assembly of *Escherichia coli* ribosomal subunits. J. Mol. Biol. **134**:1–22.
18. **Deshmukh M, et al.** 1995. Multiple regions of yeast ribosomal protein L1 are important for its interaction with 5 S rRNA and assembly into ribosomes. J. Biol. Chem. **270**:30148–30156.
19. **Deshmukh M, Tsay Paulovich Y-FAG, Woolford JL, Jr.** 1993. Yeast ribosomal protein L1 is required for the stability of newly synthesized 5S rRNA and the assembly of 60S ribosomal subunits. Mol. Cell. Biol. **13**:2835–2845.
20. **Dez C, et al.** 2004. Npa1p, a component of very early pre-60S ribosomal particles, associates with a subset of small nucleolar RNPs required for peptidyl transferase center modification. Mol. Cell. Biol. **24**:6324–6337.
21. **Dez C, Tollervey D.** 2004. Ribosome synthesis meets the cell cycle. Curr. Opin. Microbiol. **7**:631–637.
22. **Dinman JD, Icho T, Wickner RB.** 1991. A −1 ribosomal frameshift in a double-stranded RNA virus of yeast forms a gag-pol fusion protein. Proc. Natl. Acad. Sci. U. S. A. **88**:174–178.
23. **Dinman JD, Wickner RB.** 1992. Ribosomal frameshifting efficiency and gag/gag-pol ratio are critical for yeast M1 double-stranded RNA virus propagation. J. Virol. **66**:3669–3676.
24. **Dresios J, Derkatch IL, Liebman SW, Synetos D.** 2000. Yeast ribosomal protein L24 affects the kinetics of protein synthesis and ribosomal protein L39 improves translational accuracy, while mutants lacking both remain viable. Biochemistry **39**:7236–7244.
25. **Dunkle JA, Xiong L, Mankin AS, Cate JH.** 2010. Structures of the *Escherichia coli* ribosome with antibiotics bound near the peptidyl transferase center explain spectra of drug action. Proc. Natl. Acad. Sci. U. S. A. **107**:17152–17157.
26. **Dutca LM, Gallagher JE, Baserga SJ.** 2011. The initial U3 snoRNA:pre-rRNA base pairing interaction required for pre-18S rRNA folding revealed by *in vivo* chemical probing. Nucleic Acids Res. **39**:5164–5180.
27. **Egebjerg J, Leffers H, Christensen A, Andersen H, Garrett RA.** 1987. Structure and accessibility of domain I of *Escherichia coli* 23 S RNA in free RNA, in the L24-RNA complex and in 50 S subunits. Implications for ribosomal assembly. J. Mol. Biol. **196**:125–136.
28. **Emery B, de la Cruz J, Rocak S, Deloche O, Linder P.** 2004. Has1p, a member of the DEAD-box family, is required for 40S ribosomal subunit biogenesis in *Saccharomyces cerevisiae*. Mol. Microbiol. **52**:141–158.
29. **Ferreira-Cerca S, Pöll G, Gleizes PE, Tschochner H, Milkereit P.** 2005. Roles of eukaryotic ribosomal proteins in maturation and transport of pre-18S rRNA and ribosome function. Mol. Cell **20**:263–275.
30. **Ferreira-Cerca S, et al.** 2007. Analysis of the *in vivo* assembly pathway of eukaryotic 40S ribosomal proteins. Mol. Cell **28**:446–457.
31. **Fromont-Racine M, Senger B, Saveanu C, Fasiolo F.** 2003. Ribosome assembly in eukaryotes. Gene **313**:17–42.
32. **Fuentes JL, Datta K, Sullivan SM, Walker A, Maddock JR.** 2007. *In vivo* functional characterization of the *Saccharomyces cerevisiae* 60S biogenesis GTPase Nog1. Mol. Genet. Genomics **278**:105–123.
33. **Gadal O, et al.** 2001. A nuclear AAA-type ATPase (Rix7p) is required for biogenesis and nuclear export of 60S ribosomal subunits. EMBO J. **20**:3695–3704.
34. **Gadal O, et al.** 2001. Nuclear export of 60S ribosomal subunit depends on Xpo1p and requires a nuclear export sequence-containing factor, Nmd3p, that associates with the large subunit protein Rpl10p. Mol. Cell. Biol. **21**:3405–3415.
35. **Giaever G, et al.** 2002. Functional profiling of the *Saccharomyces cerevisiae* genome. Nature **418**:387–391.
36. **Grallath S, et al.** 2006. L25 functions as a conserved ribosomal docking site shared by nascent chain-associated complex and signal-recognition particle. EMBO Rep. **7**:78–84.
37. **Grandi P, et al.** 2002. 90S pre-ribosomes include the 35S pre-rRNA, the U3 snoRNP, and 40S subunit processing factors but predominantly lack 60S synthesis factors. Mol. Cell **10**:105–115.
38. **Granneman S, Petfalski E, Tollervey D.** 2011. A cluster of ribosome synthesis factors regulate pre-rRNA folding and 5.8S rRNA maturation by the Rat1 exonuclease. EMBO J. **30**:4006–4019.
39. **Harnpicharnchai P, et al.** 2001. Composition and functional characterization of yeast 66S ribosome assembly intermediates. Mol. Cell **8**:505–515.
40. **Held WA, Mizushima S, Nomura M.** 1973. Reconstitution of *Escherichia coli* 30 S ribosomal subunits from purified molecular components. J. Biol. Chem. **248**:5720–5730.
41. **Herold M, Nierhaus KH.** 1987. Incorporation of six additional proteins to complete the assembly map of the 50 S subunit from *Escherichia coli* ribosomes. J. Biol. Chem. **262**:8826–8833.
42. **Herold M, Nowotny V, Dabbs ER, Nierhaus KH.** 1986. Assembly analysis of ribosomes from a mutant lacking the assembly-initiator protein L24: lack of L24 induces temperature sensitivity. Mol. Gen. Genet. **203**:281–287.
43. **Ho JH-N, Kallstrom G, Johnson AW.** 2000. Nmd3p is a Crm1p-dependent adapter protein for nuclear export of the large ribosomal subunit. J. Cell Biol. **151**:1057–1066.
44. **Hurt E, et al.** 1999. A novel *in vivo* assay reveals inhibition of ribosomal nuclear export in Ran-cycle and nucleoporin mutants. J. Cell Biol. **144**:389–401.
45. **Jakovljevic J, et al.** Ribosomal proteins L7 and L8 function in concert with six A3 assembly factors to propagate assembly of domain I of 25S rRNA in yeast 60S ribosomal subunits. RNA, in press.
46. **Kaczanowska M, Ryden-Aulin M.** 2007. Ribosome biogenesis and the translation process in *Escherichia coli*. Microbiol. Mol. Biol. Rev. **71**:477–494.
47. **Kaiser C, Michaelis S, Mitchell A.** 1994. Methods in yeast genetics: a Cold Spring Harbor Laboratory course manual. Cold Spring Harbor Laboratory Press, Cold Spring Harbor, NY.
48. **Kemmler S, Occhipinti L, Veisu M, Panse VG.** 2009. Yvh1 is required for a late maturation step in the 60S biogenesis pathway. J. Cell Biol. **186**:863–880.
49. **Klein DJ, Moore PB, Steitz TA.** 2004. The roles of ribosomal proteins in the structure assembly, and evolution of the large ribosomal subunit. J. Mol. Biol. **340**:141–177.
50. **Kosugi S, Hasebe M, Tomita M, Yanagawa H.** 2009. Systematic identification of cell cycle-dependent yeast nucleocytoplasmic shuttling proteins by prediction of composite motifs. Proc. Natl. Acad. Sci. U. S. A. **106**:10171–10176.

51. **Kramer G, Boehringer D, Ban N, Bukau B.** 2009. The ribosome as a platform for co-translational processing, folding and targeting of newly synthesized proteins. Nat. Struct. Mol. Biol. **16**:589–597.
52. **Kressler D, de la Cruz J, Rojo M, Linder P.** 1998. Dbp6p is an essential putative ATP-dependent RNA helicase required for 60S-ribosomal-subunit assembly in *Saccharomyces cerevisiae*. Mol. Cell. Biol. **18**:1855–1865.
53. **Kressler D, Hurt E, Bassler J.** 2010. Driving ribosome assembly. Biochim. Biophys. Acta **1803**:673–683.
54. **Kruiswijk T, Planta RJ, Krop JM.** 1978. The course of the assembly of ribosomal subunits in yeast. Biochim. Biophys. Acta **517**:378–389.
55. **Lastick SM.** 1980. The assembly of ribosomes in HeLa cell nucleoli. Eur. J. Biochem. **113**:175–182.
56. **Lebreton A, et al.** 2008. 60S ribosomal subunit assembly dynamics defined by semi-quantitative mass spectrometry of purified complexes. Nucleic Acids Res. **36**:4988–4999.
57. **Lebreton A, Saveanu C, Decourty L, Jacquier A, Fromont-Racine M.** 2006. Nsa2, an unstable, conserved factor required for the maturation of 27SB pre-rRNAs. J. Biol. Chem. **281**:27099–27108.
58. **Lecompte O, Ripp R, Thierry JC, Moras D, Poch O.** 2002. Comparative analysis of ribosomal proteins in complete genomes: an example of reductive evolution at the domain scale. Nucleic Acids Res. **30**:5382–5390.
59. **Lee B, Udagawa T, Singh CR, Asano K.** 2007. Yeast phenotypic assays on translational control. Methods Enzymol. **429**:105–137.
60. **Lo KY, et al.** 2010. Defining the pathway of cytoplasmic maturation of the 60S ribosomal subunit. Mol. Cell **39**:196–208.
61. **Longtine MS, et al.** 1998. Additional modules for versatile and economical PCR-based gene deletion and modification in *Saccharomyces cerevisiae*. Yeast **14**:953–961.
62. **Mangiarotti G, Chiaberge S.** 1997. Reconstitution of functional eukaryotic ribosomes from *Dictyostelium discoideum* ribosomal proteins and RNA. J. Biol. Chem. **272**:19682–19687.
63. **Martín-Marcos P, Hinnebusch AG, Tamame M.** 2007. Ribosomal protein L33 is required for ribosome biogenesis, subunit joining, and repression of *GCN4* translation. Mol. Cell. Biol. **27**:5968–5985.
64. **Milkereit P, et al.** 2003. A Noc-complex specifically involved in the formation and nuclear export of ribosomal 40S subunits. J. Biol. Chem. **278**:4072–4081.
65. **Mizushima S, Nomura M.** 1970. Assembly mapping of 30S ribosomal proteins in *E. coli*. Nature **226**:1214–1218.
66. **Moazed D, Noller HF.** 1986. Transfer RNA shields specific nucleotides in 16S ribosomal RNA from attack by chemical probes. Cell **47**:985–994.
67. **Moritz M, Pulaski BA, Woolford JL, Jr.** 1991. Assembly of 60S ribosomal subunits is perturbed in temperature-sensitive yeast mutants defective in ribosomal protein L16. Mol. Cell. Biol. **11**:5681–5692.
68. **Mulder AM, et al.** 2010. Visualizing ribosome biogenesis: parallel assembly pathways for the 30S subunit. Science **330**:673–677.
69. **Nierhaus KH.** 1991. The assembly of prokaryotic ribosomes. Biochimie **73**:739–755.
70. **Nierhaus KH, Dohme F.** 1974. Total reconstitution of functionally active 50S ribosomal subunits from *Escherichia coli*. Proc. Natl. Acad. Sci. U. S. A. **71**:4713–4717.
71. **Nissan TA, Bassler J, Petfalski E, Tollervey D, Hurt E.** 2002. 60S pre-ribosome formation viewed from assembly in the nucleolus until export to the cytoplasm. EMBO J. **21**:5539–5547.
72. **Oeffinger M, et al.** 2007. Comprehensive analysis of diverse ribonucleoprotein complexes. Nat. Methods **4**:951–956.
73. **Ofir-Rosenfeld Y, Boggs K, Michael D, Kastan MB, Oren M.** 2008. Mdm2 regulates p53 mRNA translation through inhibitory interactions with ribosomal protein L26. Mol. Cell **32**:180–189.
74. **Ohtake Y, Wickner RB.** 1995. Yeast virus propagation depends critically on free 60S ribosomal subunit concentration. Mol. Cell. Biol. **15**:2772–2781.
75. **Peisker K, et al.** 2008. Ribosome-associated complex binds to ribosomes in close proximity of Rpl31 at the exit of the polypeptide tunnel in yeast. Mol. Biol. Cell **19**:5279–5288.
76. **Pettersen EF, et al.** 2004. UCSF Chimera-a visualization system for exploratory research and analysis. J. Comput. Chem. **25**:1605–1612.
77. **Pichon J, Marvaldi J, Marchis-Mouren G.** 1975. The *in vivo* order of protein addition in the course of *Escherichia coli* 30 S and 50 S subunit biogenesis. J. Mol. Biol. **96**:125–137.
78. **Pöll G, et al.** 2009. rRNA maturation in yeast cells depleted of large ribosomal subunit proteins. PLoS One **4**:e8249. doi:10.1371/journal.pone.0008249.
79. **Raue U, Oellerer S, Rospert S.** 2007. Association of protein biogenesis factors at the yeast ribosomal tunnel exit is affected by the translational status and nascent polypeptide sequence. J. Biol. Chem. **282**:7809–7816.
80. **Remacha M, et al.** 1995. Ribosomal acidic phosphoproteins P1 and P2 are not required for cell viability but regulate the pattern of protein expression in *Saccharomyces cerevisiae*. Mol. Cell. Biol. **15**:4754–4762.
81. **Rigaut G, et al.** 1999. A generic protein purification method for protein complex characterization and proteome exploration. Nat. Biotechnol. **17**:1030–1032.
82. **Robledo S, et al.** 2008. The role of human ribosomal proteins in the maturation of rRNA and ribosome production. RNA **14**:1918–1929.
83. **Rodríguez-Mateos M, et al.** 2009. The amino terminal domain from Mrt4 protein can functionally replace the RNA binding domain of the ribosomal P0 protein. Nucleic Acids Res. **37**:3514–3521.
84. **Rodríguez-Mateos M, et al.** 2009. Role and dynamics of the ribosomal protein P0 and its related *trans*-acting factor Mrt4 during ribosome assembly in *Saccharomyces cerevisiae*. Nucleic Acids Res. **37**:7519–7532.
85. **Rosado IV, Kressler D, de la Cruz J.** 2007. Functional analysis of *Saccharomyces cerevisiae* ribosomal protein Rpl3p in ribosome synthesis. Nucleic Acids Res. **35**:4203–4213.
86. **Sachs AB, Davis RW.** 1990. Translation initiation and ribosomal biogenesis: involvement of a putative rRNA helicase and RPL46. Science **247**:1077–1079.
87. **Sahasranaman A, et al.** 2011. Assembly of *Saccharomyces cerevisiae* 60S ribosomal subunits: role of factors required for 27S pre-rRNA processing. EMBO J. **30**:4020–4032.
88. **Sambrook J, Fritsch EF, Maniatis T.** 1989. Molecular cloning: a laboratory manual, 2nd ed. Cold Spring Harbor Laboratory Press, Cold Spring Harbor, NY.
89. **Saveanu C, et al.** 2001. Nog2p, a putative GTPase associated with pre-60S subunits and required for late 60S maturation steps. EMBO J. **20**:6475–6484.
90. **Saveanu C, et al.** 2003. Sequential protein association with nascent 60S ribosomal particles. Mol. Cell. Biol. **23**:4449–4460.
91. **Schäfer T, Strauss D, Petfalski E, Tollervey D, Hurt E.** 2003. The path from nucleolar 90S to cytoplasmic 40S pre-ribosomes. EMBO J. **22**:1370–1380.
92. **Senger B, et al.** 2001. The nucle(ol)ar Tif6p and Efl1p are required for a late cytoplasmic step of ribosome synthesis. Mol. Cell **8**:1363–1373.
93. **Shajani Z, Sykes MT, Williamson JR.** 2011. Assembly of bacterial ribosomes. Annu. Rev. Biochem. **80**:501–526.
94. **Shoji S, Dambacher CM, Shajani Z, Williamson JR, Schultz PG.** 2011. Systematic chromosomal deletion of bacterial ribosomal protein genes. J. Mol. Biol. **413**:751–761.
95. **Spillmann S, Nierhaus KH.** 1978. The ribosomal protein L24 of *Escherichia coli* is an assembly protein. J. Biol. Chem. **253**:7047–7050.
96. **Steffen KK, et al.** 2008. Yeast life span extension by depletion of 60S ribosomal subunits is mediated by Gcn4. Cell **133**:292–302.
97. **Steffen KK, et al.** 2012. Ribosome deficiency protects against ER stress in *Saccharomyces cerevisiae*. Genetics **191**:107–118.
98. **Steitz TA, Moore PB.** 2003. RNA, the first macromolecular catalyst: the ribosome is a ribozyme. Trends Biochem. Sci. **28**:411–418.
99. **Sykes MT, Shajani Z, Sperling E, Beck AH, Williamson JR.** 2010. Quantitative proteomic analysis of ribosome assembly and turnover *in vivo*. J. Mol. Biol. **403**:331–345.
100. **Takagi M, Absalon MJ, McLure KG, Kastan MB.** 2005. Regulation of p53 translation and induction after DNA damage by ribosomal protein L26 and nucleolin. Cell **123**:49–63.
101. **Talkington MW, Siuzdak G, Williamson JR.** 2005. An assembly landscape for the 30S ribosomal subunit. Nature **438**:628–632.
102. **Thomson E, Tollervey D.** 2005. Nop53p is required for late 60S ribosome subunit maturation and nuclear export in yeast. RNA **11**:1215–1224.
103. **Trapman J, Retèl J, Planta RJ.** 1975. Ribosomal precursor particles from yeast. Exp. Cell Res. **90**:95–104.
104. **Tuite MF, Stansfield I, Eurwilaichitr L, Akhmaloka.** 1993. Novel ribosome-associated translation factors are required to maintain the fidelity of translation in yeast. Biochem. Soc. Trans. **21**:857–862.
105. **Ulbrich C, et al.** 2009. Mechanochemical removal of ribosome biogenesis factors from nascent 60S ribosomal subunits. Cell **138**:911–922.
106. **van Beekvelt CA, de Graaff-Vincent M, Faber AW, van't Riet J, Venema J, Raué HA.** 2001. All three functional domains of the large ribosomal subunit protein L25 are required for both early and late pre-

rRNA processing steps in *Saccharomyces cerevisiae*. Nucleic Acids Res. **29**:5001–5008.
107. **Venema J, Planta RJ, Raué HA.** 1998. *In vivo* mutational analysis of ribosomal RNA in *Saccharomyces cerevisiae*, p 257–270. *In* Martin R (ed), Protein synthesis: methods and protocols, vol 77. Humana Press, Totowa, NJ.
108. **Venema J, Tollervey D.** 1999. Ribosome synthesis in *Saccharomyces cerevisiae*. Annu. Rev. Genet. **33**:261–311.
109. **Vilardell J, Warner JR.** 1997. Ribosomal protein L32 of *Saccharomyces cerevisiae* influences both the splicing of its own transcript and the processing of rRNA. Mol. Cell. Biol. **17**:1959–1965.
110. **Wach A, Brachat A, Alberti-Segui C, Rebischung C, Philippsen P.** 1997. Heterologous *HIS3* marker and GFP reporter modules for PCR-targeting in *Saccharomyces cerevisiae*. Yeast **13**:1065–1075.
111. **Warner JR.** 1999. The economics of ribosome biosynthesis in yeast. Trends Biochem. Sci. **24**:437–440.
112. **West M, Hedges JB, Chen A, Johnson AW.** 2005. Defining the order in which Nmd3p and Rpl10p load onto nascent 60S ribosomal subunits. Mol. Cell. Biol. **25**:3802–3813.
113. **Williamson JR.** 2009. The ribosome at atomic resolution. Cell **139**:1041–1043.
114. **Xu Z, Culver GM.** 2009. Chemical probing of RNA and RNA/protein complexes. Methods Enzymol. **468**:147–165.
115. **Yonath A.** 2005. Antibiotics targeting ribosomes: resistance, selectivity, synergism and cellular regulation. Annu. Rev. Biochem. **74**:649–679.
116. **Yu X, Warner JR.** 2001. Expression of a micro-protein. J. Biol. Chem. **276**:33821–33825.
117. **Zanchin NIT, Roberts P, DeSilva A, Sherman F, Goldfarb DS.** 1997. *Saccharomyces cerevisiae* Nip7p is required for efficient 60S ribosome subunit biogenesis. Mol. Cell. Biol. **17**:5001–5015.
118. **Zhang Y, et al.** 2010. Negative regulation of HDM2 to attenuate p53 degradation by ribosomal protein L26. Nucleic Acids Res. **38**:6544–6554.